

Synthesis of Alcohols from Carbon Oxides and Hydrogen

VIII. A Temperature-Programmed Reaction Study of *n*-Butanal on a Zn-Cr-O Catalyst

L. LIETTI, D. BOTTA, P. FORZATTI,¹ E. MANTICA, E. TRONCONI, AND I. PASQUON

Dipartimento di Chimica Industriale ed Ingegneria Chimica "G. Natta," Politecnico di Milano, Piazza Leonardo da Vinci 32, 20133 Milano, Italy

Received June 2, 1987; revised October 13, 1987

The interaction of *n*-butanal with a Zn-Cr-O catalyst has been studied by temperature-programmed reaction. Using combined GC, GC-FTIR, and GC-MS techniques, a large number of desorption products have been identified, including 1-butanol, C₈ and C₁₂ aldehydes, C₇ and C₈ ketones, and C₃, C₄, and C₇ olefins, as well as CO₂, dienes, trienes, aromatics, and light hydrocarbons. The formation of most products is explained by assuming surface reactions of two classes of intermediate species originating from the adsorption of *n*-butanal and from the surface aldol-like condensation of two molecules of *n*-butanal. Results indicate that the Zn-Cr oxide catalyst is active in performing aldehyde condensation, hydrogenation, hydrolysis, dehydrogenation, decarboxylation, and dehydration, along with isomerization and cracking reactions. Different functionalities are associated with different temperature ranges. The detected chemical functionalities are discussed with respect to their relevance to the direct synthesis of methanol and higher alcohols from CO and H₂. © 1988 Academic Press, Inc.

INTRODUCTION

Zn-Cr oxides have long been known as active and selective catalysts for the direct synthesis of methanol from CO_x and H₂ at high temperatures and pressures (1). The same catalytic systems, modified with alkali promoters, lead to the coproduction of methanol and higher alcohols (2). At present such products are of interest for their potential as octane boosters in automotive fuel blends (3-5). The industrial relevance of such a process is evident if one considers the growing limitations being placed upon the use of lead additives in gasoline for purposes of environmental protection. However, in spite of much work on Zn-Cr oxide, its catalytic behavior in the higher alcohol synthesis reaction is still far from being completely understood. A large number of reaction products, including typically linear and branched alcohols, alde-

hydes, water, carbon dioxide, methane, higher saturated and unsaturated hydrocarbons, and traces of other compounds, makes it difficult to identify the main reaction paths and to assess the origin of undesired by-products. In fact, minimizing the formation of methane and higher hydrocarbons appears crucial for the implementation of an industrial process, but this class of side reactions has not received much attention so far. Also, the well-known promoting action of alkali on the higher alcohol synthesis should be further clarified in its relationships with the main reaction pathways.

In this work we present the results of an investigation aimed at obtaining independent information on aspects of the reaction mechanism involved in the higher alcohol synthesis over Zn-Cr-O by means of the temperature-programmed surface reaction (TPSR) technique. It is well known that, during temperature-programmed desorption into an inert carrier stream, a single

¹ To whom correspondence should be addressed.

adsorbate can decompose or react on the catalyst surface to yield several products. Valuable information on surface reaction mechanisms and kinetics can be extracted from the desorption spectra of the reaction products and of the unreacted adsorbate (6). If suitable operating parameters are selected, intermediate species can in principle be desorbed and detected as soon as they form, making this technique very attractive for mechanistic investigations. On the other hand, TPSR experiments are performed at near-atmospheric pressure, while the higher alcohol synthesis is carried out under moderate to high pressures. Thus, care should be exercised in relating directly the results of TPSR runs to the catalytic behavior under real synthesis conditions. Nevertheless, the TPSR technique can successfully identify a number of catalytic functions of the investigated systems. TPSR of different molecules, including CO, CO + H₂, CO₂, H₂O, CH₃OH, HCHO, HCOOH, C₁–C₄ linear and branched alcohols, C₁–C₂ aldehydes, and ethers, over several oxides, such as ZnO, MgO, SiO₂, and metals, have been reported (7–13). The characteristics identified include dehydrogenation and dehydration as well as decomposition to CO and H₂, which appear to depend on both the catalytic system and the nature of the adsorbed molecule.

It has been proposed that the overall reaction network of the higher alcohol synthesis over modified high-temperature methanol catalysts involves a series of consecutive steps, namely formation of C₁ species, formation of a carbon–carbon bond to yield C₂ compounds, and chain growth to higher oxygenated products, possibly involving aldehydic intermediates. Likewise, proposed mechanisms leading to the formation of hydrocarbons either imply independent routes (e.g., a Fischer–Tropsch mechanism) or share steps with the mechanism responsible for the formation of oxygenates: for example, this would be the case if hydrocarbons derive primarily from a consecutive alcohol dehydration. The picture

would be better clarified if one could avoid most of the numerous reaction products and focus on a few primary reaction steps. Accordingly, C₄ compounds, which are the oxygenated higher products formed in the largest amounts under typical synthesis conditions, were considered potentially most informative for a TPSR investigation on prereduced Zn–Cr–O samples. The purpose was twofold: on the one hand the aim was to assess the chemical functionalities involved in the interaction with a Zn–Cr–O system, in order to gain independent information on its catalytic behavior under reaction conditions; on the other hand it was thought that TPSR experiments would be helpful in determining whether C₄ oxygenated compounds are indeed terminal products, or whether they can be involved in secondary reactions, possibly associated with the further chain growth of alcohols and/or with the formation of hydrocarbons. This work is concerned with TPSR of *n*-butanal; the behavior of branched C₄ aldehydes and of linear and branched C₄ alcohols is being investigated at present and will be reported in subsequent papers. The effect of alkali addition will also be addressed.

EXPERIMENTAL

The apparatus used for the temperature-programmed surface reaction experiments is shown schematically in Fig. 1. Helium was used as the carrier gas, with a typical flow rate of 100 cm³/min under STP conditions controlled by Brooks 5850 mass flow regulators. A cylindrical quartz reactor was used, with a reactor design similar to that discussed by Falconer and Schwarz (14). The reactor is narrow (i.d., 5 mm) so that radial temperature gradients are minimized. The temperature of the catalyst bed was raised according to a linear heating schedule by use of a Eurotherm Model 812 programmer and PID regulator, the heating rate being 10°C/min during all runs up to 450°C. The temperature was measured by means of a Chromel–Alumel thermocouple

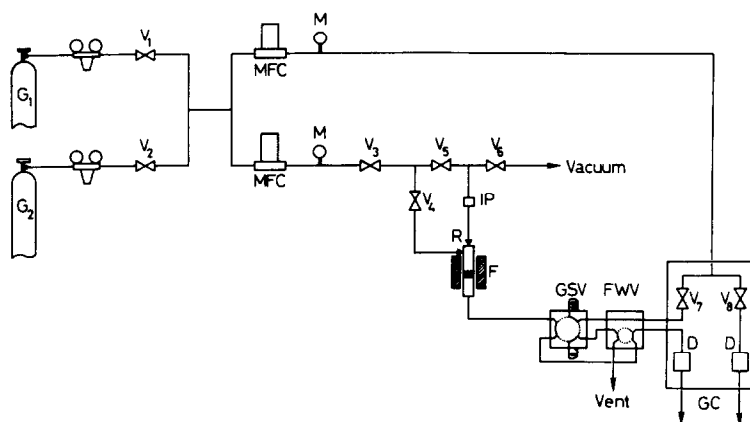


FIG. 1. Schematic diagram of the TPSR apparatus: G_1 and G_2 , gas cylinders (1, helium; 2, reducing mixture); V, valves; MFC, mass flow controller; M, manometer; IP, injection point; R, reactor; F, furnace; GSV, gas sampling valve; FWV, four-way valve; GC, gas chromatograph; D, detector.

directly immersed in the catalyst bed. All tubes and connections downstream from the reactor were heated to prevent condensation of the desorbed species.

Each TPSR run was started with a fresh catalyst sample. A commercial Zn–Cr–O catalyst was used, with a Zn/Cr atomic ratio of 3 and a BET surface area of 120 m²/g. The sample (0.150 g), ground and sieved at 120–200 mesh to minimize internal diffusional limitations, was pretreated *in situ* at 450°C for 25 min in flowing N₂ with 5% H₂ (flow rate, 100 cm³/min). After cooling to room temperature, the N₂–H₂ mixture was replaced by He, switching off valve V₂ and opening valve V₁. Then, pulses of aldehyde were passed on the catalyst bed at 35°C through a dedicated line until saturation was achieved. The reactor, still at 35°C, was then evacuated at 1.3×10^{-3} bar for 15 min to remove the weakly physisorbed molecules. After adsorption and evacuation the carrier gas was allowed to flow over the catalyst bed for 20 min, and then the TPSR run was begun.

During a typical TPSR experiment the quartz reactor was connected to a flame ionization detector (FID) from a Carlo Erba FTV 2350 gas chromatograph, with no separation column inserted in the line. The concentration of the desorbing compounds in the carrier gas stream was continuously

monitored, from which overall TPSR traces were obtained.

After completion of the run, each TPSR experiment was repeated with a fresh catalyst sample. During the repeated runs, the nature and the amount of the desorbing compounds were determined by two distinct analytical procedures. The first one involved condensation in a –196°C liquid-nitrogen-cooled trap containing a few microliters of CS₂ and located immediately downstream from the reactor (15). Upon warming to r.t., a CS₂ solution was obtained, which was then analyzed by GC, GC-FTIR, and GC-MS. The GC analyses were performed on capillary columns with different phases (OV1, SE 54, PS 255). Typical conditions for GC, GC-FTIR, and

TABLE I
GC Analysis Conditions

Gas chromatograph: Carlo Erba FTV 2150 modified for capillary column.
Column: Fused silica capillary column coated with OV 1 as stationary phase. i.d., 0.33 mm; length, 25 m; film thickness, 3 μm.
Carrier gas: Helium at 2 cm ³ /min.
Injection: Split (split ratio 1/30) or splitless. T_{inj} = 250°C. Sample quantity: 1 μl of CS ₂ solution.
Oven temperature: Isothermal 30°C for 15 min, 30 → 250°C at 4°C/min.

TABLE 2

GC and Fourier Transform IR Analysis Conditions

Gas chromatography
Gas chromatograph: Carlo Erba Mega 5160.
Column: Fused silica capillary column coated with SE 54 silicone rubber. i.d., 0.33 mm; length, 50 m; film thickness, 0.3 μ m.
Carrier gas: Helium at 2 cm ³ /min.
Injection: Cold on-column. Sample quantity, 1 μ l of CS ₂ solution.
Oven temperature: Isothermal 30°C for 10 min, 30 \rightarrow 250°C at 3°C/min.
Fourier transform IR spectroscopy
FTIR spectrophotometer: Nicolet 60 SX.
Frequency range: 4000–700 cm ⁻¹ , resolution 8 cm ⁻¹ .
IR source: water cooled Globar (reference source: Laser HeNe).
Beam splitter: KBr coated with Ge.
GC-FTIR interface: Nicolet with stainless-steel glass-coated transfer lines (230°C) and glass tubular gold-coated cell (i.d., 1 mm; length, 150 mm; KBr windows; 230°C).
Make-up gas: He, 2 cm ³ /min.
Detector: MCT-A liquid-nitrogen cooled.
Data System: High-speed Nicolet 1280 computer.

GC-MS analysis are reported in Tables 1, 2, and 3.

The second procedure was based on on-line gas chromatographic analysis. In this case the carrier gas line was modified switching on valve V₇ and selecting the sampling valves so as to bypass the GC, and samples of the carrier gas containing the desorbed species were periodically analyzed using a gas sampling valve and a Porapak QS separation column 4 m long (100–120 mesh) inserted in the GC. The heating program included 30 min at 120°C followed by heating up to 180°C (heating rate, 2°C/min). The on-line gas chromatographic analyses were usually performed by a FI detector, but a TC detector was also employed to assess the presence of CO (in combination with a molecular sieve column), CO₂, and H₂O in the effluent gas stream.

The two different but complementary analytical procedures enabled the detection and identification of both light and heavy products in complex mixtures. The former

procedure secured integral data and allowed the detection of condensable species; the latter enabled us to follow the evolution with temperature of more volatile species.

Reproducibility of TPSR experiments and of the associated analyses was found satisfactory based on replicated runs. Chromatographic helium and *n*-butanal Carlo Erba RPE reagent were used during all runs.

After TPSR experiments the catalyst samples were characterized by DTA-TG analysis under O₂ and N₂ in order to assess the presence of carbon species adsorbed on the catalyst surface. DTA-TG data were obtained by a Mettler 2000 instrument typically operating with a heating rate of 20°C/min.

The catalytic activity of the Zn–Cr–O sample was tested in a fixed bed tubular reactor operated at *T* = 405°C, *P* = 85 atm, H₂/CO = 1/1, GHSV = 8000 h⁻¹. Details on the experimental setup for activity runs are provided elsewhere (5).

RESULTS

The TPSR trace of *n*-butanal following adsorption at 35°C is shown in Fig. 2. Two

TABLE 3

GC-MS Analysis Conditions

Instrument: GC-MS Hewlett–Packard Model 5985 B.
Gas chromatograph: Hewlett–Packard Model 5940 A modified for capillary column.
Column: Fused silica capillary column coated with SE 54 silicone rubber. i.d., 0.33 mm; length, 50 m; film thickness, 0.3 μ m.
Carrier gas: Helium at 2 cm ³ /min.
Injection: Splitless. <i>T</i> _{inj} = 250°C. Sample quantity, a 1 μ l of CS ₂ solution.
Oven temperature: Isothermal 30°C for 10 min, 30 \rightarrow 250°C at 3°C/min.
Interface GC-MS: The capillary column was directly introduced in the ion source. Transfer line, 260°C.
MS: Hyperbolic quadrupole mass filter.
Source: Dual source EI/CI. <i>T</i> _{source} = 200°C. Electron energy 70 eV.
Detector: Electron multiplier at 2200 V.
Data System: HP 21 MX series E computer.

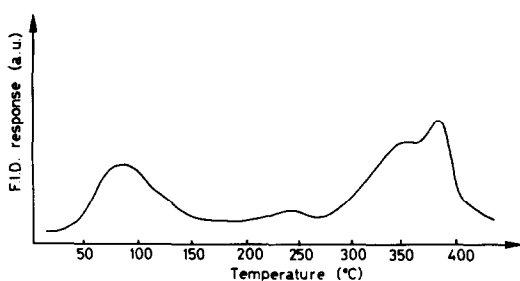


FIG. 2. TPSR trace of *n*-butanol from the Zn-Cr-O sample.

maxima with $T_M = 89^\circ\text{C}$ and 383°C and shoulders at about 130°C and 350°C are evident, together with a weak maximum at 250°C .

The compounds desorbed into the carrier gas stream up to 200°C , corresponding to the first peak in the overall TPSR trace, have been condensed and analyzed by GC, GC-FTIR, and GC-MS. The results of the gas chromatographic analysis are presented in Fig. 3. The most relevant IR and MS features of the main detected species, and their relative amounts, are given in Table 4. As is apparent from Fig. 3, a number of additional compounds were also detected, although in traces, originating from reagent impurities or secondary surface reactions. The on-line FID GC analyses confirmed that no other lighter products were present in this range of temperatures.

Inspection of Table 4 shows that relatively small amounts of the reactant, *n*-butanol, and of the corresponding alcohol, 1-butanol, were desorbed. As indicated by on-line GC analysis, the alcohol/aldehyde molar ratio increased with temperature. The most abundant compound observed was 2-ethyl-2-hexenal; small amounts of an isomeric species with an identical mass spectrum, but a slightly higher retention time, were also observed. The other primary reaction products identified were 4-heptanone and an aldehyde with molecular peak $m/e = 180$ amu, possibly a doubly unsaturated C_{12} aldehyde.

The high-temperature peak ($T_M = 383^\circ\text{C}$) results from the desorption of various products. The species desorbed in the temperature range 250 – 410°C , corresponding to the second peak of the overall TPSR trace, have been condensed and analyzed by GC, GC-FTIR, and GC-MS. Figure 4 shows the results of the gas chromatographic analysis. The proposed identification of these compounds is reported in Table 5. In this case, the on-line gas chromatographic analysis provided complementary results, as it allowed detection of a number of additional lighter products. The overall quantitative analysis is presented in Table 6. Note that *n*-butanol and 1-butanol were no longer detected. The primary products associated with the second TPSR peak are propylene

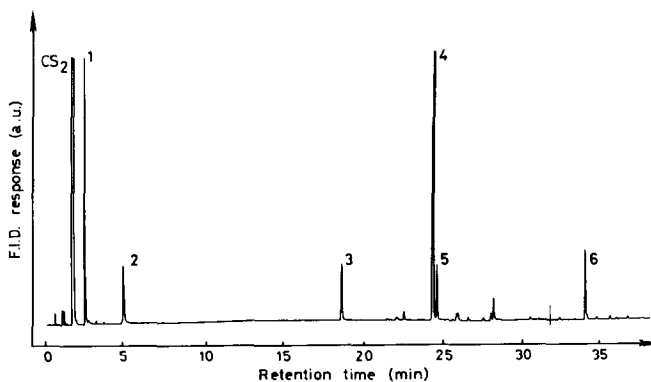


FIG. 3. GC analysis of the compounds desorbed up to 200°C and condensed in the CS_2 trap at -196°C .

TABLE 4

Analysis of the TPSR Products Desorbed in the Range 30–200°C and Condensed in the CS₂ Trap at –196°C

Peak No.	FTIR features ^c	Mass spectrum <i>m/e</i> (% intensity) ^d	Proposed identification	Relative amount ^a (%)
1	—		<i>n</i> -Butanal ^a	17.
2	—		1-Butanol ^a	12.
3	$\nu_{\text{C-H}}(\text{CH}_2, \text{CH}_3)$ at 2850–2959 cm ^{–1} (s) $\nu_{\text{C=O}}$ at 1729 cm ^{–1} (s)	71(100) 43(77) 114 ^m (45) 41(30) 39(16)	4-Heptanone	5.
4	$\nu_{\text{C-H}}(\text{CH}_2, \text{CH}_3)$ at 2850–2964 cm ^{–1} (s) $\nu_{\text{C-H}}(\text{—C=O})$ at 2802(m), 2711(m) cm ^{–1} H $\nu_{\text{C=O}}$ at 1707 cm ^{–1} (vs)	55(100) 41(65) 97(60) 126 ^m (51) 39(40) 111(28) 69(20) 83(19)	2-Ethyl-2-hexenal	60.
5	—	^b	Isomer of 2-ethyl-2-hexenal	3.
6	$\nu_{\text{C-H}}(\text{CH}_2, \text{CH}_3)$ at 2850–2968 cm ^{–1} (s) $\nu_{\text{C-H}}(\text{—C=O})$ at 2805(m), 2710(m) cm ^{–1} H $\nu_{\text{C=O}}$ at 1740 cm ^{–1} (s)	137(100) 67(82) 151(80) 109(75) 43(42) 81(40) 180 ^m (35) 55(32) 123(23) 165(21) 95(13)	Doubly unsaturated C ₁₂ aldehyde	3.

^a On the basis of GC analysis.^b Similar to that of peak No. 4.^c vs, very strong; s, strong; m, medium; w, weak.^d m, molecular peak.

and C₇ linear olefins. All of the five possible isomers, namely 1-heptene, *trans*-2-heptene, *cis*-2-heptene, *trans*-3-heptene, and *cis*-3-heptene, were identified. Significant amounts of butenes (1-butene and/or isobutene, *cis*-2-butene and *trans*-2-butene) were also observed, together with slightly smaller quantities of ethylene, C₅ hydrocar-

bons, and C₈ dienes. 4-Heptanone, a C₈ ketone along with two unsaturated isomeric C₈ species, C₇ dienes, toluene, C₅–C₆ ketones, and C₉–C₁₆ aromatics were also detected. Figure 5 illustrates the evolution with temperature of the main compounds, as obtained by on-line gas chromatographic analysis. It is apparent that

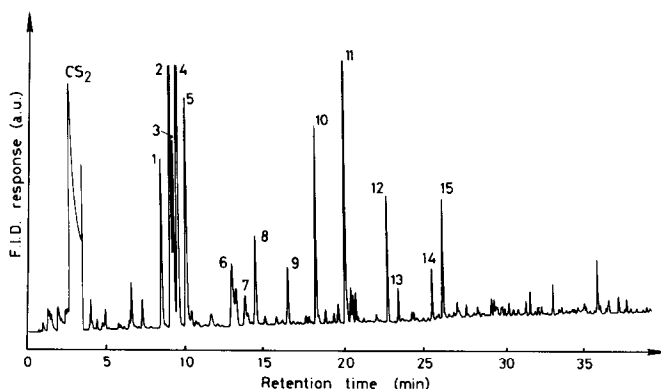


FIG. 4. GC analysis of the compounds desorbed in the temperature range 250–410°C and condensed in the CS₂ trap at –196°C.

TABLE 5

Analysis of the TPSR Products Desorbed in the Range 250–410°C and Condensed in the CS₂ Trap at –196°C


Peak No.	FTIR features ^a	Mass spectrum <i>m/e</i> (% intensity) ^b	Proposed identification
1	$\nu_{C-H}(=CH_2)$ at 3087 cm ⁻¹ (w) $\nu_{C-H}(CH_2, CH_3)$ at 2850–2936 cm ⁻¹ (s) δ_{CH_2, CH_3} antisym at 1450 cm ⁻¹ (w) δ_{CH_3} sym at 1371 cm ⁻¹ (w) $\gamma_{CH}(=C-H)$ at 904 cm ⁻¹ (w) 	41(100) 56(86) 55(84) 39(81) 70(53) 69(37) 42(30) 98 ^m (28) 57(25) 83(9)	1-Heptene
2	$\nu_{C-H}(=CH)$ at 3015 cm ⁻¹ (w) $\nu_{C-H}(CH_2, CH_3)$ at 2850–2940 cm ⁻¹ (s) δ_{CH_2, CH_3} antisym at 1459 cm ⁻¹ (w) $\gamma_{C-H}(=)$ at 964 cm ⁻¹ (w)	41(100) 55(66) 56(65) 98 ^m (63) 69(62) 39(58) 53(22) 70(16) 83(5)	<i>trans</i> -3-Heptene
3	$\nu_{C-H}(=CH)$ at 3020 cm ⁻¹ (w) $\nu_{C-H}(CH_2, CH_3)$ at 2850–2940 cm ⁻¹ (s) δ_{CH_2, CH_3} antisym at 1459 cm ⁻¹ (w)	41(100) 56(72) 98 ^m (66) 55(66) 39(58) 69(52) 55(22) 70(17) 83(5)	<i>cis</i> -3-Heptene
4	$\nu_{C-H}(=CH)$ at 3015 cm ⁻¹ (w) $\nu_{C-H}(CH_2, CH_3)$ at 2850–2940 cm ⁻¹ (s) δ_{CH_2, CH_3} antisym at 1459 cm ⁻¹ (w) $\gamma_{C-H}(=)$ at 957 cm ⁻¹ (w)	55(100) 41(78) 56(73) 39(63) 98 ^m (62) 69(37) 53(22) 70(16) 83(4)	<i>trans</i> -2-Heptene
5	$\nu_{C-H}(=CH)$ at 3015 cm ⁻¹ (m) $\nu_{C-H}(CH_2, CH_3)$ at 2850–2940 cm ⁻¹ (s) δ_{CH_2, CH_3} antisym at 1461 cm ⁻¹ (w)	55(100) 56(89) 41(81) 98 ^m (73) 39(71) 69(48) 53(26) 70(22) 83(5)	<i>cis</i> -2-Heptene
6	$\nu_{C-H}(=CH)$ at 3010 cm ⁻¹ (w) $\nu_{C-H}(CH_2, CH_3)$ at 2850–2967 cm ⁻¹ (s) δ_{CH_2, CH_3} antisym at 1455 cm ⁻¹ (w) δ_{CH_3} sym at 1370 cm ⁻¹ (w) $\gamma_{C-H}(=)$ at 971 cm ⁻¹ (m)	81(100) 96 ^m (50) 79(42) 53(27) 39(26) 67(25) 41(20) 55(13) 51(12)	C ₇ diene
7	$\nu_{C-H}(Ar-H)$ at 3022 cm ⁻¹ (m) $\nu_{C-H}(CH_3)$ at 2850–2923 cm ⁻¹ (m)	91(100) 92 ^m (58) 39(9) 51(9) 65(9)	Toluene
8	$\nu_{C-H}(CH_2, CH_3)$ at 2850–2968 cm ⁻¹ (s) $\nu_{C=O}$ at 1733 cm ⁻¹ (s)	57(100) 43(90) 100 ^m (70) 71(70) 41(40) 39(28) 42(17) 55(10) 85(5)	C ₆ ketone
9	$\nu_{C-H}(=CH_2)$ at 3078 cm ⁻¹ (w) $\nu_{C-H}(=CH)$ at 3020 cm ⁻¹ (w) $\nu_{C-H}(CH_2, CH_3)$ at 2850–2950 cm ⁻¹ (s)	68(100) 67(82) 95(42) 53(36) 39(32) 41(32) 79(18) 81(17) 110 ^m (10)	C ₈ diene
10	$\nu_{C-H}(=CH)$ at 3015 cm ⁻¹ (w) $\nu_{C-H}(CH_2, CH_3)$ at 2850–2968 cm ⁻¹ (s) δ_{CH_2, CH_3} antisym at 1461 cm ⁻¹ (w) δ_{CH_3} sym at 1375 cm ⁻¹ (w) $\gamma_{C-H}(=)$ at 951 cm ⁻¹ (w)	95(100) 110 ^m (80) 81(77) 67(73) 79(42) 39(40) 53(40) 55(34) 41(31) 68(26)	C ₈ diene
11	$\nu_{C-H}(CH_2, CH_3)$ at 2850–2960 cm ⁻¹ (s) $\nu_{C=O}$ at 1730 cm ⁻¹ (s)	71(100) 43(77) 114 ^m (45) 41(30) 39(16)	4-Heptanone
12	$\nu_{C-H}(CH_2, CH_3)$ at 2850–2960 cm ⁻¹ (s) $\nu_{C=O}$ at 1719 cm ⁻¹ (m) δ_{CH_2, CH_3} antisym at 1451 cm ⁻¹ (w) δ_{CH_3} sym at 1371 cm ⁻¹ (w)	71(100) 57(88) 43(65) 41(56) 128 ^m (43) 85(26) 39(23) 100(15)	C ₈ saturated ketone
13	$\nu_{C-H}(=CH)$ at 3015 cm ⁻¹ (w) $\nu_{C-H}(CH_2, CH_3)$ at 2964 cm ⁻¹ (s) $\nu_{C-H}(CH_2, CH_3)$ at 2870 cm ⁻¹ (m) $\nu_{C=O}$ at 1693 cm ⁻¹ (s)	55(100) 83(100) 43(25) 97(23) 39(20) 41(15) 111(15) 53(13) 126 ^m (11) 98(10) 71(8)	C ₈ unsaturated ketone

TABLE 5—(Continued)

Peak No.	FTIR features ^a	Mass spectrum <i>m/e</i> (% intensity) ^b	Proposed identification
14	$\nu_{\text{C-H}}(\text{CH}_2, \text{CH}_3)$ at 2870–2968 cm^{-1} (s) $\nu_{\text{C-H}}(\text{—C=O})$ at 2796(w), 2701(w) cm^{-1} $\begin{array}{c} \text{H} \\ \\ \text{C=O} \end{array}$ $\nu_{\text{C=O}}$ at 1706 cm^{-1} (vs)	55(100) 41(65) 97(60) 126 ^m (51) 39(40) 111(28) 69(20) 83(19)	2-Ethyl-2-hexenal
15	$\nu_{\text{C-H}}(\text{=CH}_2)$ at 3080 cm^{-1} (w) $\nu_{\text{C-H}}(\text{CH}_2, \text{CH}_3)$ at 2850–2965 cm^{-1} (s) $\nu_{\text{C=O}}$ at 1686 cm^{-1} (s)	83(100) 55(90) 111(50) 39(15) 53(10) 41(9) 43(9) 126 ^m (2)	C ₈ unsaturated ketone

^a vs, very strong; s, strong; m, medium; w, weak.^b m, molecular peak.

the desorption of 4-heptanone, and particularly of the C₇ olefins, causes the appearance of the shoulder at 350°C in the overall TPSR trace. Likewise, desorption of propylene is mainly responsible for the peak at 383°C. The evolution of butenes begins earlier, roughly corresponding to the intermediate weak maximum at 250°C, and occurs rather uniformly up to the highest temperatures. C₂ and C₅ hydrocarbons were detected only at higher temperatures, along

with traces of CH₄, not given in Fig. 5. Altogether, the compounds represented in Fig. 5 account for about 90% of the overall desorbed products.

The data obtained using a TC detector showed the presence of CO₂ and H₂O in the gas stream at 300°C, and of CO₂ at 336°C. CO₂ was always present in comparable amounts with propylene + C₇ linear olefins. These results are consistent with the shape of the overall TPSR trace recorded by the TC detector. When compared to the corresponding trace obtained using a FID, in fact, the TC curve exhibits a very similar first peak, but a different shape with a more pronounced maximum is observed for the

TABLE 6

Quantitative Analysis of the TPSR Products
Desorbed in the Range 250–450°C

Products	Relative amount ^a (%)
Propylene	39.4
C ₇ linear olefins	21.7
Butenes	9.4
C ₅ hydrocarbons	5.8
Ethylene	5.2
4-Heptanone	4.0
C ₈ dienes	3.8
C ₉ –C ₁₆ unsaturated	
Hydrocarbons (aromatics)	3.0
C ₇ dienes	2.0
C ₈ saturated ketone	1.3
C ₈ unsaturated ketones	1.3
C ₅ –C ₆ ketones	1.6
Toluene	1.0
2-Ethyl-2-hexenal	0.5

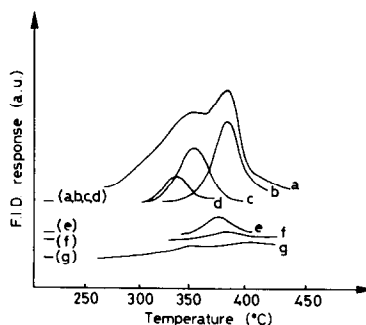
^a On the basis of GC analysis.

FIG. 5. TPSR traces of the compounds desorbed in the high-temperature region: (a) overall TPSR trace; (b) propylene; (c) C₇ linear olefins; (d) 4-heptanone; (e) C₅ hydrocarbons; (f) ethylene; (g) butenes.

TABLE 7
Results of Activity Runs over the Pure and K-Promoted Zn-Cr-O Sample

Sample	% CO conv.	Productivities (g/liter h)					Average N _c	
		CH ₃ OH	CH ₄	CH ₃ OCH ₃	C ₂₊ oxy.	C ₂₊ hyd.	C ₂₊ oxy.	C ₂₊ hyd.
ZnCrO _x	6.8	63.3	27.1	51.5	6.6	14.3	4.0	2.6
ZnCrO _x + 3% K ₂ O	10.7	71.8	11.9	5.0	128.0	32.6	4.1	3.0

Note. Reaction conditions: $T = 405^{\circ}\text{C}$; $P = 85\text{ atm}$; $\text{H}_2/\text{CO} = 1/1$; $\text{GHSV} = 8000\text{ h}^{-1}$.

second peak, owing to desorption of species undetectable by FID.

DTA-TG analysis under an O₂ atmosphere of samples of the Zn-Cr-O catalyst after TPSR runs indicated a small weight loss (0.3%) associated with an exothermic peak ($T_M = 275^{\circ}\text{C}$). Such effects were not observed either under N₂ or during DTA-TG of a sample subjected to a TPSR cycle with no adsorbate, i.e., pretreatment up to 450°C for 25 min in flowing N₂ with 5% H₂, cooling down to room temperature, and subsequent treatment in He up to 450°C for 25 min.

Table 7 shows the results of the catalytic activity tests over the pure and K-promoted Zn-Cr-O catalyst under conditions typical of the higher alcohol synthesis. Both samples exhibited good activity toward methanol formation. Although rather poor, the catalytic function responsible for the formation of C₂₊ oxygenates was also manifest over the unpromoted sample. A product distribution with an average carbon number of 4.0 was measured. The addition of K to the catalyst promoted dramatically the formation of higher oxygenated products, but did not affect significantly their average carbon number. Considerable amounts of dimethyl ether, methane, olefins, and hydrocarbons (mostly C₂ and C₃) were also observed among the products. Alkali addition depressed the formation of dimethyl ether by an order of magnitude, and to a lesser extent the formation of methane, while C₂₊ hydrocarbons were more abundant in this case. Small amounts of methyl

formate and other esters, as well as ketones, were detected in the product mixture.

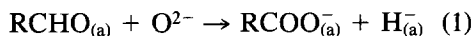
DISCUSSION

TPSR of *n*-Butanal

Among the products detected during the TPSR runs a great number of compounds have been identified that do not originate from simple adsorption followed by desorption or decomposition of *n*-butanal: this clearly points to the occurrence of surface chemical reactions on the Zn-Cr-O sample.

Most of the observed reaction products can be explained by assuming the presence of two classes of intermediate surface species represented in Figs. 6 and 7, originating from the adsorption of *n*-butanal (species A₁, A₂, A₃), and from the surface aldol-like condensation of two aldehyde molecules (species B₁, B₂, B₃), respectively. These species appear to describe the origin of the detected products, as shown schematically in Figs. 6 and 7 and discussed in the following.

Species similar to A₁ and A₂ are typically observed upon interaction of an aldehyde molecule with oxidic surfaces. The molecularly adsorbed species A₁ is formed by interaction of *n*-butanal with a Lewis acid site. The carboxylate ion is produced according to the oxidative dehydrogenation reaction (16)



Such a reaction possibly operates once

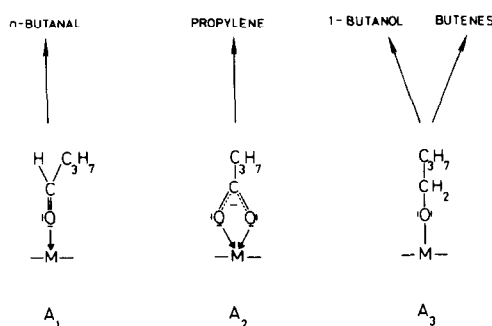
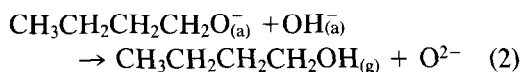


FIG. 6. Intermediate surface species originating from the adsorption of *n*-butanal, and products desorbed therefrom.

the prerduced catalyst surface is depleted of hydrogen. The alkoxide species can already be formed at room temperature by reduction of the molecularly adsorbed aldehyde by H_2 adsorbed during catalyst pretreatment. An alternate route involving a Cannizzaro-type disproportionation reaction of a surface dioxymethylene intermediate, leading to species A_2 and A_3 , is also possible. As a matter of fact, a dioxymethylene species has been observed by IR following adsorption of HCHO on a number of ionic oxides; this species undergoes a Cannizzaro disproportionation to methoxy groups and formate ions (17–20). Moreover, an acetal intermediate has been proposed as the result of the interaction of acetaldehyde with the ZnO surface by Bowker *et al.* (11).

Species A_1 is reversible in nature and accounts for the desorption of *n*-butanal in the low-temperature region.

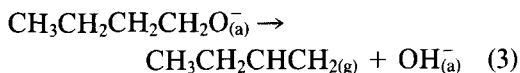
The desorption of 1-butanol involves the following surface reaction of species A_3 ,



in line with previous proposals advanced for methanol and ethanol desorption (21, 22). The ratio 1-butanol/*n*-butanal grows with increasing temperature, probably for kinetic reasons.

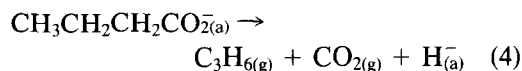
At higher temperatures, roughly corresponding to the intermediate weak TPSR

peak at $T_M = 250^\circ\text{C}$, dehydration of species A_3 begins to occur, resulting in the evolution of butenes according to



Our analyses has indicated the presence of 1-butene and/or isobutene (it was not possible to separate these isomers), *cis*-2-butene and *trans*-2-butene. Butenes were also reported among the products detected during TPD of 1-butanol from ZnO (13).

Finally, the considerable amounts of propylene observed in the high-temperature TPSR peak are explained by a decarboxylation reaction of species A_2 . Such a species is strongly interacting with the catalyst surface and undergoes decomposition at high temperatures according to the reaction



Indeed, large quantities of CO_2 were detected in the carrier gas stream in the same temperature range where propylene desorbs. A similar mechanism has been suggested (11) to account for the decomposition of acetate groupings. The large amounts of propylene as compared to 1-butanol plus butenes confirm that reaction (1) is primarily responsible for the formation of carboxylate ions.

The surface aldol-like condensation of two aldehyde molecules is tentatively assumed to result in species B_1 , B_2 , and B_3 shown in Fig. 7.

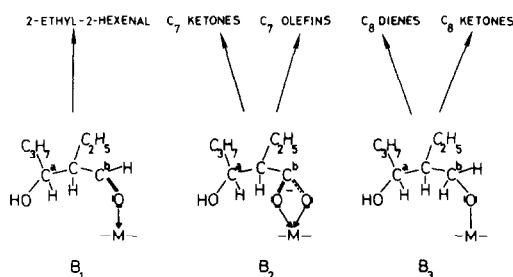


FIG. 7. Intermediate surface species originating from the aldol-like condensation of two *n*-butanal molecules, and products desorbed therefrom.

The aldolic condensation of acetone to mesityl oxide over α -Fe₂O₃ was observed by IR (23). The proposed mechanism requires a deprotonating capacity of the surface, resulting in the formation of the enolate anion of acetone, which further reacts with gaseous acetone to give diacetone alcohol. Mesityl oxide is then produced by dehydration of diacetone alcohol. A similar mechanism can be invoked to account for the formation of species B₁ at low temperatures. As already discussed for species of class A, in addition to the molecularly adsorbed species, the corresponding carboxylate and alkoxy species are likely to be present.

Species B₁, B₂, and B₃ can be linked directly to the origin of the following among the several C₇ and C₈ observed desorption products: 2-ethyl-2-hexenal, 4-heptanone, C₇ linear olefins, C₈ ketones, C₈ dienes.

Formation of 2-ethyl-2-hexenal is explained by dehydration of species B₁, followed by desorption. On the other hand, decarboxylation of species B₂, followed by dehydrogenation on the C^a carbon atom and by keto-enol tautomerism, leads to the desorption of 4-heptanone. A similar mechanism is expected to operate during the synthesis of acetone from ethanol over a number of oxides including ZnO-Cr₂O₃ which has been recently reported by Nakajima *et al.* (24). C₇ linear olefins are obtained by decarboxylation of species B₂ with dehydration. The C₈ saturated ketones observed among the desorbed products are likely to result from dehydration on the C^b carbon atom of species B₃, followed by double-bond migration and keto-enol tautomerism. Finally, desorption of C₈ dienes is associated with dehydration on both C^a and C^b carbon atoms of the same species.

The aldol-like condensation reaction involving three *n*-butanal molecules can also account for the detection of doubly unsaturated C₁₂ aldehyde.

The scheme proposed so far accounts for >90% of the gas chromatographic area corresponding to the analysis of all the de-

sorbed species. A few extra species have been identified, which can be associated with consecutive surface reactions of the primary products. Thus, the C₇ linear olefins apparently undergo dehydrogenation reactions, resulting in C₇ dienes. Traces of C₇ trienes were also observed, but these species probably act as intermediates in a further aromatization to toluene.

Also, C₉-C₁₆ unsaturated hydrocarbons, primarily aromatics, following a nearly uniform distribution, and C₅-C₆ ketones were desorbed. It may be reasonably supposed that these species originate from the fragmentation and transformation of surface intermediates with greater molecular weight than that of species B₁, B₂, and B₃, resulting from further condensation reactions.

The formation of light hydrocarbons (C₁, C₂, C₃) observed at higher temperatures is best explained by cracking. The relevance of the cracking reactions of heavy products grows with temperature, as expected. In fact the on-line GC analysis shows that near the end of the TPSR run only light hydrocarbons are detected, while there is no longer evidence of heavy products. Furthermore, the catalyst is subject to fouling during the TPSR experiments: carbon species resulting from cracking are left on the catalyst surface and are rapidly oxidized in the course of the DTA-TG analysis. The exothermic peak of the DTA curve is not easily explained otherwise. In fact,

(i) if it were simply due to the oxidation of the catalyst sample, it would be associated with a weight gain, not with a weight loss;

(ii) the exothermic peak was not observed during DTA of a sample that went through the whole TPSR procedure but with no adsorbate.

Catalyst Functions

This study has demonstrated the capability of the TPSR technique, when coupled to adequate analytical facilities, to point out characteristic chemical functionalities of catalytic systems. In the case of Zn-Cr-O,

these results can provide valuable insight into the complex behavior of similar catalysts when operated under actual reaction conditions for the direct synthesis of methanol and higher alcohols from syngas. Accordingly, such functions are discussed in the following in the light of their relevance to the synthesis reaction.

It is worth mentioning that most of the same properties were identified during a related TPSR study of isobutanol (25). On the other hand, some differences were detected when the C_4 aldehydes were replaced by C_4 alcohols (1-butanol and isobutanol) as the adsorbate (25, 26). Such differences are illustrated in the discussion of the following points.

(a) *Aldol-like condensation*. The condensation product of *n*-butanal, 2-ethyl-2-hexenal, has been observed already in the low-temperature region; also, there is strong analytical evidence for the formation of a further condensation product, a doubly unsaturated C_{12} aldehyde. The capability of the Zn–Cr–O system, not modified by alkali addition, to promote aldolic condensations, is worth noting. Actually, compounds with more than four carbon atoms are predominant among the desorbed species. On the other hand, during TPSR of both 1-butanol and isobutanol, compounds originating from C_8 or higher precursors were never observed.

In the early literature chain growth mechanisms for the higher alcohol synthesis over modified methanol catalysts based on condensations of either alcohols (27) or aldehydes (28) were proposed. Our results provide evidence in favor of a chain growth mechanism based on successive condensations of aldehydes. A similar reaction scheme had been proposed by Morgan *et al.* (28) to explain the C_{2+} product distribution of the higher alcohol synthesis over a K-promoted Mn–Cr–O catalyst.

The data of the catalytic activity tests (see Table 7) confirm that the chain growth capability is equally active over both the unpromoted and the K-promoted Zn–Cr–O

sample, yielding similar higher alcohol distributions with the same average carbon number. However, the overall content of C_{2+} oxygenates is much greater in the case of the K-promoted sample, thus pointing to a slow $C_1 \rightarrow C_2$ step, followed by a fast further chain growth. The role of the alkali dopants is apparently that of accelerating the slow initial step rather than the subsequent condensations.

(b) *Hydrogenation*. The desorption of 1-butanol and butenes from prerduced Zn–Cr–O catalysts has been related to the presence of a C_4 alkoxy species, which can originate either by hydrogenation of the molecularly adsorbed *n*-butanal or by a Cannizzaro-type disproportionation of a surface dioxybutylidene intermediate. In the higher alcohol synthesis the hydrogenation function is probably exploited in the reduction of aldehydes to the corresponding alcohols, the aldehydes being the products of the aldolic condensation mechanism for chain growth discussed above. Under high H_2 partial pressures, typical of synthesis conditions, additional hydrogenation reactions are likely to become apparent, including for example the conversion of olefins to saturated hydrocarbons.

On the other hand, a disproportionation function can be invoked to account for the minor amounts of methyl formate observed under reaction conditions.

(c) *Hydrolysis and alcoholysis*. The desorption of 1-butanol from an *n*-butoxy intermediate occurs through a hydrolysis reaction. This function may be involved in the formation of alcohols under reaction conditions. A similar function, namely, alcoholysis, can be invoked to explain the presence of ethers in the reaction products.

(d) *Dehydrogenation*. The formation of dienes, trienes, and aromatics from the corresponding olefins, as well as the production of 4-heptanone and propylene by decarboxylation, requires a dehydrogenation function. Actually, it is well known that many materials are good catalytic agents for both hydrogenation and dehydrogena-

tion, depending on the operating conditions. Under typical synthesis reaction conditions the dehydrogenation functionality is likely to be minimized by the conspicuous H_2 partial pressures involved.

(e) *Decarboxylation*. This is one of the most evident functions of the Zn–Cr–O catalyst pointed out by the TPSR study at high temperatures. Both intermediate species A_2 and B_2 were subject to decarboxylation. Under synthesis conditions, however, this reaction is expected to occur to a much lesser extent due to the high H_2 partial pressure, which inhibits the oxidative dehydrogenation of the molecularly adsorbed aldehyde species to the corresponding carboxylate ions.

(f) *Dehydration*. The formation of a number of desorbed products observed during TPSR experiments involves a dehydration step. This function is likely to be active also under actual synthesis conditions. It is responsible for the large amounts of dimethyl ether formed over the unpromoted Zn–Cr–O sample (see Table 7) and may be partially responsible also for the production of hydrocarbons. In this respect, some confirming evidence can be found in the literature: for example, Frohlich and Cryder (29) reported that, upon adding ethanol to a H_2 /CO feed mixture passed over a Zn–Mn–Cr–K–O catalyst at about 200 atm and 400°C, a good part of it was dehydrated to ethylene. Anderson *et al.* (30) invoked an alcohol dehydration mechanism to explain the temperature dependence of the product distribution observed in the so-called “iso-synthesis” over Th oxide catalysts, where isobutanol was the main C_{2+} product observed below 400°C, whereas isobutene and isobutane (and generally hydrocarbons) were predominant at higher temperatures.

Note that alkali addition essentially suppresses the dehydration activity leading to ether formation, as demonstrated in Table 7. In the case of hydrocarbons such an effect is not evident, possibly due to the corresponding large increase in the concentrations of higher alcohols which can undergo dehydration.

(g) *Isomerization*. Migration of the C=C double bond appears to be easy over the Zn–Cr–O sample under TPSR conditions, since typically a number of isomers have been identified for both hydrocarbon and oxygenated unsaturated compounds. Due to limitations of the analytical facilities, it was not possible to collect evidence for the occurrence of skeletal isomerization in the case of *n*-butanal as well as in the case of 1-butanol.

Under reaction conditions the isomerization function is reflected in the formation of isomers of olefins (e.g., 1- and 2-butenes).

(h) *Cracking*. At high temperatures there are clear indications for the onset of cracking reactions. This function is associated with strong acidic catalyst surface sites and is expected to be minimized by alkali addition. The relevance of these reactions under typical synthesis conditions is presently under investigation.

ACKNOWLEDGMENTS

This work was supported by Progetto Finalizzato Energetica/2. Thanks are also due to Dr. G. Busca for useful discussion.

REFERENCES

1. Natta, G., in “Catalysis” (P. H. Emmett, Ed.), Vol. III, p. 349. Reinhold, New York, 1955.
2. Natta, G., Colombo, U., and Pasquon, I., in “Catalysis” (P. H. Emmett, Ed.), Vol. V, p. 131. Reinhold, New York, 1957.
3. Italian Patent 25390 to Snamprogetti (December 2, 1981).
4. U.S. Patent 4,513,100 to Snamprogetti (April 23, 1985).
5. Tronconi, E., Ferlazzo, N., Forzatti, P., and Pasquon, I., *Ind. Eng. Chem.* **26**, 2122 (1987).
6. Madix, R. J., in “Advances in Catalysis” (D. D. Eley, H. Pines, and P. B. Weisz, Eds.), Vol. 29, p. 1. Academic Press, New York, 1980.
7. Benziger, J. B., and Madix, R. J., *J. Catal.* **65**, 36 (1980).
8. Sexton, B., Rendulic, K. D., and Hughes, A. E., *Surf. Sci.* **121**, 181 (1980).
9. Rendulic, K. D., and Sexton, B. A., *J. Catal.* **78**, 126 (1982).
10. Noller, H., and Ritter, G., *J. Chem. Soc. Faraday Trans. 1* **80**, 275 (1984).
11. Bowker, M., Houghton, H., and Waugh, K. C., *J. Catal.* **79**, 431 (1983).

12. Bowker, M., Petts, R. W., and Waugh, K. C., *J. Chem. Soc. Faraday Trans.* **81**, 3073 (1985).
13. Bowker, M., Petts, R. W., and Waugh, K. C., *J. Catal.* **99**, 53 (1986).
14. Falconer, J. L., and Schwarz, J. A., *Catal. Rev. Sci. Eng.* **25**, 141 (1983).
15. Witte, K., and Dissinger, O., *Z. Anal. Chem.* **236**, 119 (1968).
16. Lorenzelli, V., Busca, G., and Sheppard, N., *J. Catal.* **66**, 28 (1980).
17. He, M. Y., and Ekerdt, J. G., *J. Catal.* **90**, 17 (1984).
18. Lavalley, J. C., Lamotte, J., Busca, G., and Lorenzelli, V., *J. Chem. Soc. Chem. Commun.*, 1005 (1985).
19. Busca, G., Lamotte, J., Lavalley, J. C., and Lorenzelli, V., *J. Amer. Chem. Soc.*, in press.
20. Busca, G., Elmi, A. S., and Forzatti, P., *J. Phys. Chem.* **91**, 5263 (1987).
21. Klier, K., "Advances in Catalysis" (D. D. Eley, H. Pines, and P. B. Weisz, Eds.), Vol. 31, p. 243. Academic Press, New York, 1981.
22. Bowker, N., Houghton, H., and Waugh, K. C., *J. Chem. Soc. Faraday Trans. 1* **78**, 2573 (1982).
23. Busca, G., and Lorenzelli, V., *J. Chem. Soc. Faraday Trans. 1* **78**, 2911 (1982).
24. Nakajima, T., Yamaguchi, T., and Tanabe, K., *J. Chem. Soc. Chem. Commun.*, 394 (1987).
25. Unpublished results from our laboratories.
26. Lietti, L., Tronconi, E., and Forzatti, P., *J. Mol. Catal.* **44**, 201 (1987).
27. Graves, G. D., *Ind. Eng. Chem.* **23**, 1381 (1931).
28. Morgan, G. T., Hardy, D. V. N., and Procter, R. H., *J. Soc. Chem. Ind. Trans. Commun.* **51**, 1T (1932).
29. Frohlich, P. K., and Cryder, D. S., *Ind. Eng. Chem.* **22**, 1051 (1930).
30. Anderson, R. B., Feldman, J., and Storch, H. H., *Ind. Eng. Chem.* **44**, 2418 (1952).